AIP Publishing

This manuscript was accepted by Rev. Sci.Instrum. Click here to see the version of record.

High voltage performance of a dc photoemission electron gun with centrifugal barrel-polished electrodes

C. Hernandez-Garcia, D. Bullard, F. Hannon, Y. Wang and M. Poelker
Jefferson Lab, Newport News, VA 23693, USA

The design and fabrication of electrodes for direct current (dc) high voltage photoemission electron guns can significantly influence their performance, most notably in terms of maximum achievable bias voltage. Proper electrostatic design of the triple point junction shield electrode minimizes the risk of electrical breakdown (arcing) along the insulator-cable plug interface, while the electrode shape is designed to maintain < 10 MV/m at the desired operating voltage aiming at little or no field emission once conditioned. Typical electrode surface preparation involves diamond paste polishing by skilled personnel, requiring several weeks of effort per electrode. In this work, we describe a centrifugal barrel-polishing technique commonly used for polishing the interior surface of superconducting radio frequency cavities but implemented here for the first time to polish electrodes for dc high voltage photoguns. The technique reduced polishing time from weeks to hours while providing surface roughness comparable to that obtained with diamond-paste polishing and with unprecedented consistency between different electrode samples. We present electrode design considerations and high voltage conditioning results to 360 kV (~11 MV/m), comparing barrel-polished electrode performance to that of diamond-paste polished electrodes. Tests were performed using a dc high voltage photogun with an inverted-geometry ceramic insulator design.

ACCEPTED MANUSCRIPT

I. INTRODUCTION

Today's dc high voltage photoemission guns require electrodes capable of operating at 100-400 kV and at field strengths of the order 10 MV/m to provide high brightness electron beams for accelerator applications that require high bunch charge such as free electron lasers[1], energy recovery linacs[2] and electron-cooling[3]. It is essential that electrodes exhibit little or no field emission during continuous operation at these voltages[4,5]. Low-level field emission at nano-Ampere levels desorbs gas from the vacuum chamber walls by direct impact and by x-ray stimulated desorption, leading to enhanced ion bombardment of the photocathode which hastens quantum efficiency decay[6]. Field emission at the micro-Ampere level can lead to high voltage breakdown that completely eliminates photocathode quantum efficiency, and in some instances can result in irreparable damage of the photogun insulator[7].

Buffered chemical polishing and electropolishing are state-of-the-art polishing techniques used to polish the large interior surfaces of superconducting radio frequency accelerating cavities[8]. These techniques have been implemented to polish electrodes for dc high voltage photoguns with encouraging results[9,10]. Wet chemical techniques speed the polishing of electrodes compared to labor intensive diamond-paste polishing (DPP), however wet-chemical techniques possess an unappealing level of subjectivity, namely related to the specific concentrations of chemicals used in the etching solution and the amount of time the electrode remains in the chemical bath[11]. If implemented incorrectly, wet chemical polishing techniques can damage the electrode, for example leaving a mottled and rough finish. Another disadvantage of wet chemical polishing

AIP Publishing

This manuscript was accepted by Rev. Sci.Instrum. Click here to see the version of record.

relates to the significant removal of material that is inherent to the process – the removal of 100 µm from the surface is typical, but can be difficult to precisely control. Material removal must be considered at the time of design and fabrication. Too little or too much material removed from the part can affect how electrode pieces fit together and how the electrode attaches to the ceramic insulator. Small gaps can significantly influence the achieved field strength at critical locations on the electrode surface.

In search of a reliable and time-efficient alternative to DPP and the wet chemical polishing methods mentioned above, we have demonstrated successful implementation of centrifugal barrel-polishing (also known as tumbling) of stainless steel electrodes with ~200 cm^2 surface area, manufactured for a dc high voltage photogun designed to operate at 350 kV (10.5 MV/m peak). With tumbling, the resulting surface roughness was comparable to that attained with DPP, while the polishing time was significantly reduced from weeks to hours. The behavior of the electrode during high voltage conditioning was similar to electrodes polished via DPP. We describe the polishing technique and present a surface-analysis comparison of DPP-ed and CBP-ed samples. We also present important design considerations related to the electrode shape and the electrode-insulator interface particular to the inverted-insulator geometry employed at Jefferson Lab as a test bed for the barrel polished electrodes. This is the first implementation of the tumbling technique for the construction and operation of a 350kV dc high voltage photogun.

II. MECHANICAL AND HV DESIGN

A. Inverted geometry ceramic insulator and vacuum chamber

A number of dc high voltage photoguns rely on large cylindrical ceramic insulators to electrically isolate the cathode electrode[12,13,14], which must be supported on a long coaxial metal support structure. In contrast to these designs, an inverted-insulator geometry design was chosen at Jefferson Lab for two reasons: First to provide a smaller volume which could result in better achievable vacuum because there is less surface area to contribute a gas load; and second, the insulator serves as the electrode support structure which means there is less metal biased at high voltage, and less metal to contribute to field emission[15,16,17].

The photogun described in this work is a larger version of the 130 kV dc high voltage photogun used at the Continuous Electron Beam Accelerator Facility (CEBAF)[16]. The cylindrical vacuum chamber design shown in figure 1 is relatively compact, 45 cm diameter, and with volume and surface area approximately one third of photogun designs with large cylindrical insulators that operate at comparable voltage.

The 15.25 cm diameter cathode electrode was manufactured using two hydroformed hemispherical shells (316L stainless steel) that were welded together. The narrow end of the conical insulator passes through a hole in the cathode electrode and mates to an internal fixture that holds the photocathode puck (Figure 1). The spherical electrode possesses a front face with 1.2 cm opening and 25° Pierce focusing geometry. Spring-loaded sapphire rollers push the photocathode puck against the back of the focusing faceplate. Interior components of the electrode are held in place using a rear face plate that also smooths the electrostatic field.

ACCEPTED MANUSCRIPT

AIP Publishing

This manuscript was accepted by Rev. Sci.Instrum. Click here to see the version of record.

The spherical cathode electrode attaches to a conical ceramic insulator[18] suspended from a 25 cm Conflat flange. For the purpose of the high voltage tests described in this work, a molybdenum "puck" with a polished stainless steel wafer was inserted into the cathode electrode via a vacuum load-lock using a long-arm magnetic manipulator[15].

There are five holes in the anode plate. The photoemitted electron beam passes through the large center hole and the other holes provide a means to deliver laser light to the photocathode at 25° angle of incidence and to pass the unabsorbed reflected light outside the photogun. The anode is electrically isolated from ground using sapphire balls, to provide a means to measure incident field emission and to bias the anode to repel downstream ions created by the beam[19].

The bottom half of the gun chamber is lined with an array of eight non-evaporable getter pump modules (SAES WP1250 with ST707 material) to provide an estimated pump speed of ~4000 l/s for hydrogen, which is the dominant gas species inside the vacuum chamber. A perforated ground screen covers the NEG modules to minimize the likelihood that NEG particulate becomes electrostatically charged, and attracted to the cathode electrode initiating field emission[12]. An adjustable leak valve mounted to the side of the photogun vacuum chamber provides a means to krypton gas-condition the electrode when field emission is encountered[7].

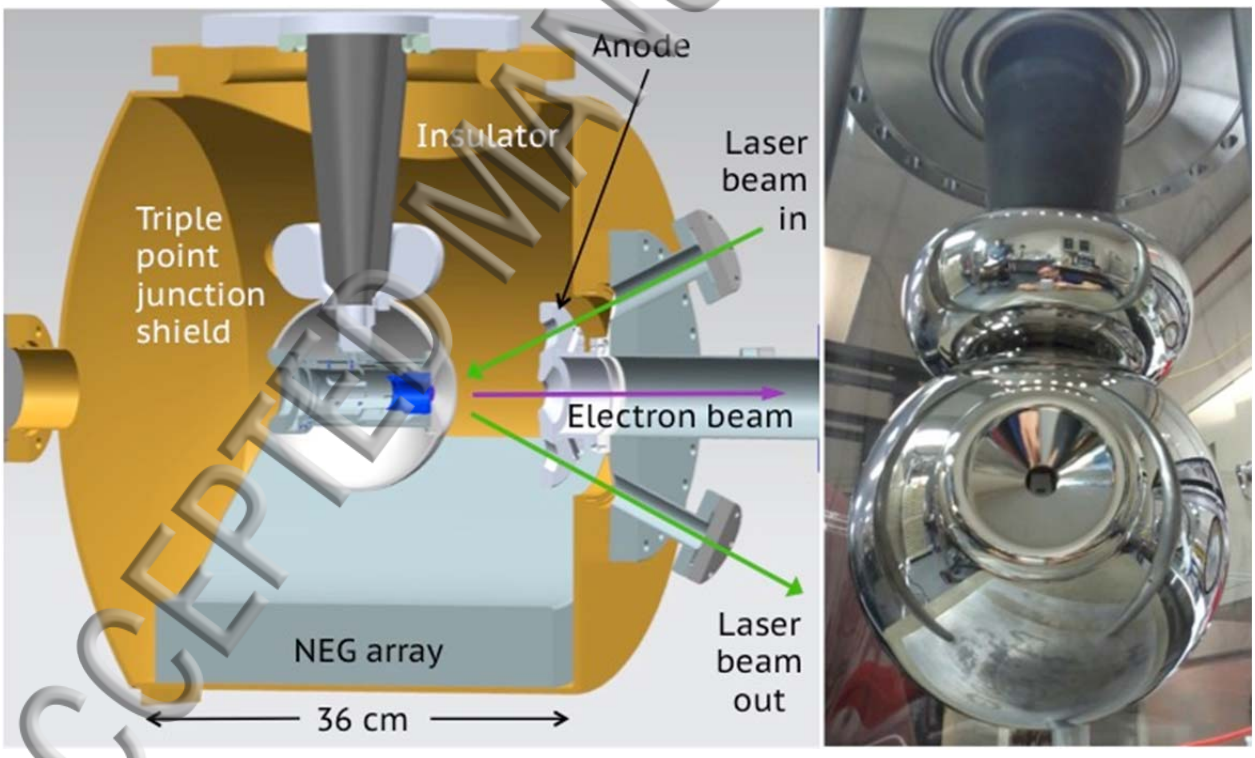

FIG. 1. Left: Cross-section view of the 350kV photogun with inverted geometry ceramic insulator (dark grey). The photocathode (purple) and puck (blue) sit inside the 15.25 cm diameter spherical cathode electrode with 25° Pierce focusing angle. Right: Photograph of the CBP-ed stainless steel spherical electrode attached to the doped alumina inverted-geometry ceramic insulator welded to a 25 cm Conflat flange.

B. Electrode HV design

ACCEPTED MANUSCRIPT

AIP Publishing

This manuscript was accepted by Rev. Sci.Instrum. Click here to see the version of record.

A previous study highlighted the most significant drawback of the inverted insulator design, namely one of the triple-point junctions resides at high voltage[17]. As a result, great care must be taken to properly design the triple-point junction at the high voltage end of the inverted insulator to avoid arcing discharges to ground and resultant catastrophic failure of the insulator. A properly designed triple-point junction shield serves to minimize the electric field at the ceramic-metal-vacuum interface and creates a linear potential gradient along the insulator. In addition, a doped insulator with lower resistivity than a conventional pure alumina insulator provided improved high voltage performance. The dopant gives the insulator a dark grey appearance (Figure 1), and serves to drain charge that might build-up within the bulk or on the surface of the insulator as a result of direct impact of field emitted electrons, and by electron-hole pair production from x-rays when field emitted electrons impact the vacuum chamber walls.

Electrostatic field maps were obtained using the Poisson Superfish electrostatic solver[20]. Iterative adjustments to the electrostatic model served to optimize the diameter of the cathode electrode within the gun chamber, set the cathode-anode gap, and to refine the shape of the triple-point junction shield with goal of keeping the electric field strength less than ~ 10 MV/m at 350kV bias voltage. Higher dc field strengths often lead to field emission that can be very difficult to process out[7]. The Poisson Superfish electrostatic solver is ideally suited for configurations with cylindrical geometry. The photogun has two axes of symmetry: the vertical axis defined by the insulator, and the longitudinal axis defined by the electron beam path in the anode-cathode gap (Figure 1). The high voltage analysis of the insulator and plug including corresponding dielectric properties, and the design of the triple-point junction shield were performed using cylindrical symmetry, while the anode-cathode gap optimization was done using Cartesian coordinates[17].

After setting the anode-cathode gap at 9 cm to achieve an electric field strength of ~ 10 MV/m at 350kV bias voltage, consideration was given to the design of the triple junction screening electrode, based on the criteria shown below, and with the intention of keeping field strength values less than 10 MV/m everywhere on the entire surface, for a bias voltage of 350 kV[17]. Figure 2 shows the equipotential lines and electric field strength values of the optimized triple junction screening electrode design.

a) Vary the gap and the contour near the triple-point junction to minimize the electric field strength both parallel and perpendicular to the surface of the insulator by adjusting the triple-point junction shield height, and by tapering its contour away from the insulator near the triple-point junction. Field-emitted electrons from the triple-point junction can initiate pre-breakdown currents that often lead to arcing along the ceramic insulator at the cable-plug interface.
b) Adjust the height of the triple-point junction shield to minimize the electric field at the triple junction while keeping the contour field strength less than 10 MV/m at 350kV. The height of the triple-point junction shield influences the potential along the insulator, especially at the insulator-high voltage plug interface. A “taller” triple-point junction shield will create a more linear potential gradient, but it will increase the field strength at the top because it has moved closer to the vacuum chamber wall.

ACCEPTED MANUSCRIPT

This manuscript was accepted by Rev. Sci.Instrum. Click here to see the version of record.

c) Adjust the outermost radius of the triple-point junction shield, maintaining a radius smaller than the spherical electrode radius, in order to minimize distortions to the radial and longitudinal electric field within the anode-cathode gap.

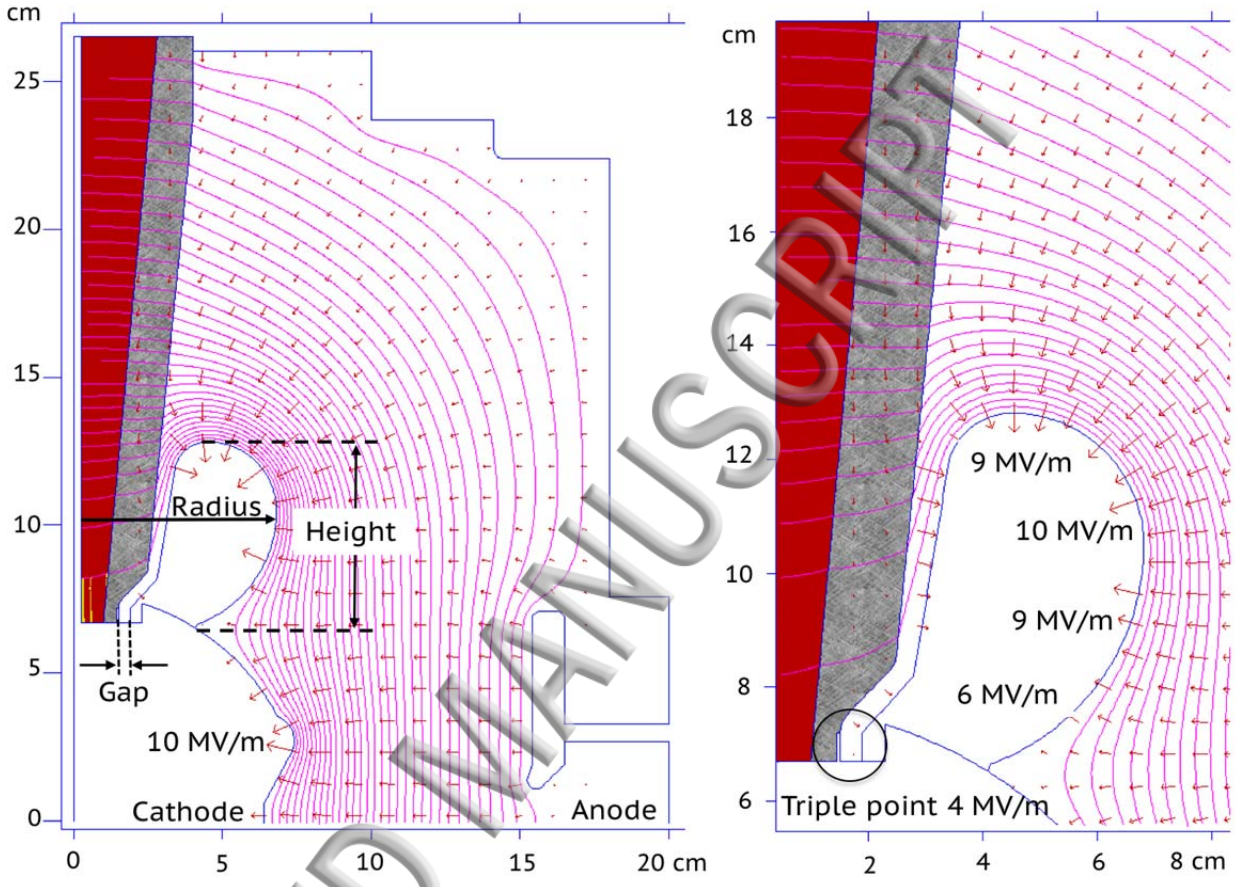

FIG. 2. Left: Electrostatic field map showing the insulator, screening and spherical electrodes, and anode-cathode gap modeled with the electrostatic solver Poisson Superfish, the pink lines are the equipotentials at 350 kV, the doped alumina insulator is shown in grey, and the rubber cable plug in maroon. Right: Close-up view of the triple-point junction screening electrode at 350 kV, the circle indicates the ceramic-metal-vacuum triple-point junction and the field strength.

III. ELECTRODE SURFACE PREPARATION AND CHARACTERIZATION

A. Barrel polishing

The commercial centrifugal barrel polishing machine[21] employs plastic barrels filled with dry polishing media, in which the electrode was immersed. The machine used at Jefferson Lab holds up to four barrels that are attached to a spinning drum (Figure 3). Viewed from the side, the configuration looks like a Ferris wheel. As the drum rotates in one direction, the barrels rotate in the opposite direction which causes the media and parts rub against one another randomly and repeatedly. When only one part is polished, the barrel polishing machine requires a counter

ACCEPTED MANUSCRIPT

AIP Publishing

This manuscript was accepted by Rev. Sci.Instrum. Click here to see the version of record.

weight. The polishing time depends on electrode size and mass, which are important factors in the polishing process. Two types of polishing media were suggested by the vendor, plastic cones and crushed corncob. Although each media can be used multiple times, for this study fresh media was used during each polishing interval. And to prevent cross contamination from residue, each media had its own barrel. Between polishing intervals, the part was wiped clean with lint-free tissue soaked in 2-propanol prior to immersion in the fresh media-filled barrel.

FIG. 3. Top: Centrifugal barrel polishing machine used to polish the photogun electrodes. Bottom: plastic cones and corncob polishing media.

Electrodes and accompanying test samples were manufactured with "32" finish specification, meaning 32 micro-inches roughness average surface finish, equivalent to ~ 0.8 microns. The roughness average ($R_a = \frac{1}{L}\int_0^L |Z(x)|\, dx$), known as the arithmetic mean, represents the average of all peak and valley deviations $Z(x)$ from a centerline across a sampling line of length L. After manufacture, each electrode was vacuum degassed at 900° C and then polished using the following procedure:

1) Fill barrel with plastic cones to approximately 30% capacity (9/16" RTC #200 Cones[21]).
2) Place electrode in the barrel and cover with plastic cones to the 70% capacity line.

ACCEPTED MANUSCRIPT

AIP Publishing

This manuscript was accepted by Rev. Sci.Instrum. Click here to see the version of record.

3) Add diluted cleaning solution to 70% capacity (4 liquid ounces of TS Cleaning Compound M[21] per 1 gallon of water).
4) Secure barrel in the polishing machine and rotate at 100 RPM for X minutes.
5) Remove electrode from barrel and clean with lint-free tissue soaked in 2-propanol.
6) Immerse the electrode in another barrel filled to 70% capacity with dry corn cob polishing media (MF-3 Fine Treated Corn Cob[21]).
7) Secure barrel in the polishing machine and rotate at 100 RPM for Y minutes.
8) Remove electrode from barrel and clean in ultrasonic baths in the following sequence: diluted degreaser Micro-90, de-ionized water, 2-propanol and final rinse de-ionized water.

The polishing times for each media were initially suggested by the vendor based on sample size and mass and then refined empirically. For example, to achieve a similar surface finish using plastic cones, the triple junction screening electrode with mass ~ 0.6 kg required 30 minutes, whereas the spherical shell electrode with mass ~ 0.1 kg required 60 minutes. Polishing longer, beyond the empirically determined minimum duration, did not improve or damage the surface finish. In one instance, a spherical electrode was polished with corn cob media for 24 hours (because this sample was inside a barrel used as a counter-weight while an SRF cavity was being polished). Upon visual examination, the surface appeared to be identical to that of another spherical shell electrode polished with corncob for only 30 minutes.

Figure 4 shows the evolution of the surface finish of the triple junction screening electrode as received from the machine shop, after 30 minutes polishing with plastic cones, and after subsequent 30 minutes polishing with corncob media. The machine tooling marks were completely removed by the plastic cones.

ACCEPTED MANUSCRIPT

AIP Publishing

This manuscript was accepted by Rev. Sci.Instrum. Click here to see the version of record.

FIG. 4. Photographs show the evolution of the surface finish of the triple junction screening electrode. Top: as received form the machine shop with 32 finish. Center: after 30 minutes of CBP using plastic cones. Bottom: final result after 30 minutes of CBP with plastic cones followed by 30 minutes with corncob.

ACCEPTED MANUSCRIPT

B. Surface characterization

AIP Publishing

This manuscript was accepted by Rev. Sci.Instrum. Click here to see the version of record.

Surface finish was evaluated by measuring the roughness average Ra using two non-contact methods: optical profilometry with a Veeco WYKO NT1100 Optical Profiling System, and atomic force microscopy (AFM) with a Nanoscope Dimension 3100. The optical profilometry measurements were performed on two types of samples: 20 cm^2 stainless steel anode electrode disks, and 1 cm^2 stainless steel test "coupons". The optical profilometer sampling area was approximately 0.5 cm^2 and the device could accommodate large parts like the anode electrodes.

Figure 5 shows optical profilometry results of the two sample types, anode electrodes and coupons. Figures 5a, 5b, 5d and 5e show the effectiveness of the barrel polishing with plastic cones in removing machine tooling marks and in producing a consistent finish regardless of initial surface conditions. The anode disc was pre-polished with 320-grit sandpaper (Fig. 5a), while the coupons were not (Fig. 5d). Even though the initial Ra was a factor of 4 higher for the coupon (Ra=850 nm) compared to the anode disc (Ra=185 nm), the resultant Ra for both samples was very similar after barrel polishing with plastic cones (Fig. 5b, anode disc Ra=182 nm, and Fig 5e, coupon Ra=185 nm). The anode disc was polished in each media for 30 minutes (like the more massive photogun screening electrode), while the coupons were polished for 60 minutes in each media (like the less massive spherical cathode electrode). Figures 5b and 5e illustrate how CBP with plastic cones produces a homogenous surface finish, effectively removing the initial tooling marks clearly visible across the surface of the coupon. Similarly, and even though the anode disc Ra did not improve significantly, polishing with plastic cones served to homogenize the pre-polished surface with 320-grit sandpaper. Barrel polishing with cones renders a consistent, homogenous surface finish regardless of the initial surface condition. After final polishing with corn cob media (Fig. 5c, anode disc Ra=76 nm, and Fig. 5f, coupon Ra=48 nm), the Ra values of the anode electrode and coupon were comparable to Ra values (~30 nm) of DPP-ed stainless steel electrodes[9].

ACCEPTED MANUSCRIPT

AIP Publishing

This manuscript was accepted by Rev. Sci.Instrum. Click here to see the version of record.

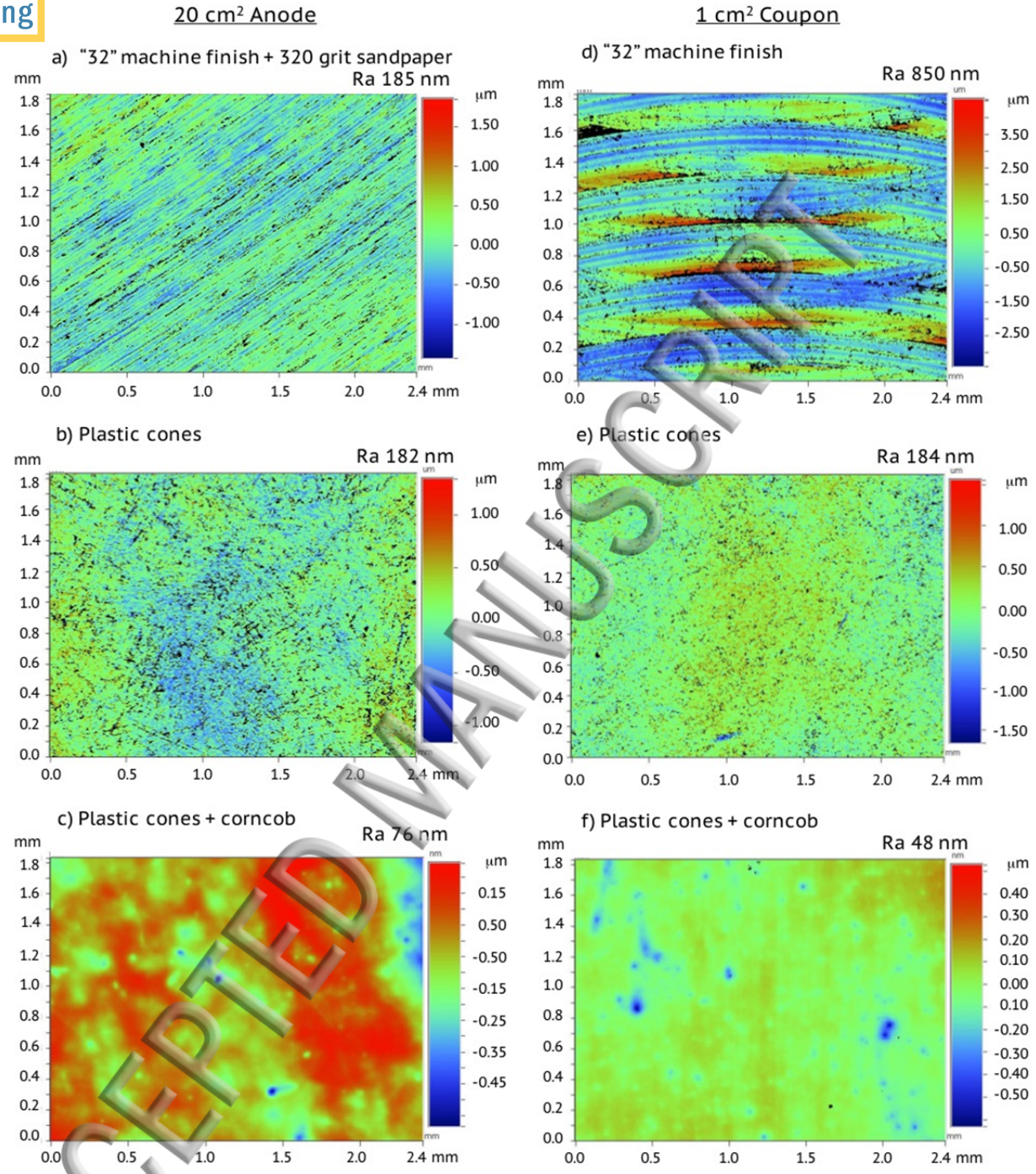

FIG. 5. False-color optical profilometer images showing the surface profile with corresponding surface finishing method and surface roughness average measurement on the 20 cm^2 stainless steel anode [(a), (b), (c)] and on 1 cm^2 stainless steel coupons [(d), (e), (f)]. The sampling area is ~ 0.5 cm^2.

Further analysis of the coupons using the AFM showed that the surface finish Ra was ~ 50 nm (Figure 6 Top) after tumbling in plastic cones and ~ 6 nm (Figure 6 Bottom) after subsequent tumbling in corncob. The AFM sampling area was of the order of 25 μm^2 and was limited to evaluation of smaller parts, i.e., the coupons. The roughness average measurements of

ACCEPTED MANUSCRIPT

AIP Publishing

This manuscript was accepted by Rev. Sci.Instrum. Click here to see the version of record.

centrifugal barrel polished samples and comparisons with DPP techniques are summarized in Table 1. The results show that the surface roughness attained with the centrifugal barrel polishing techniques described in this work is comparable to DPP-ed stainless steel coupons[22]. Note that surface roughness Ra values measured with the AFM are smaller than those obtained with optical profilometry. This is because submicron details are smoothed out by the optical profilometer since it has lower spatial resolution than the AFM[23]. Other factors contributing to the differences in Ra results between the two non-contact methods may be attributed to effects of scan size, sampling interval, region studied, etc. for each instrument. Despite the differences, results from both the optical profilometer and the AFM show that the surface finish progressively improves with each polishing media step.

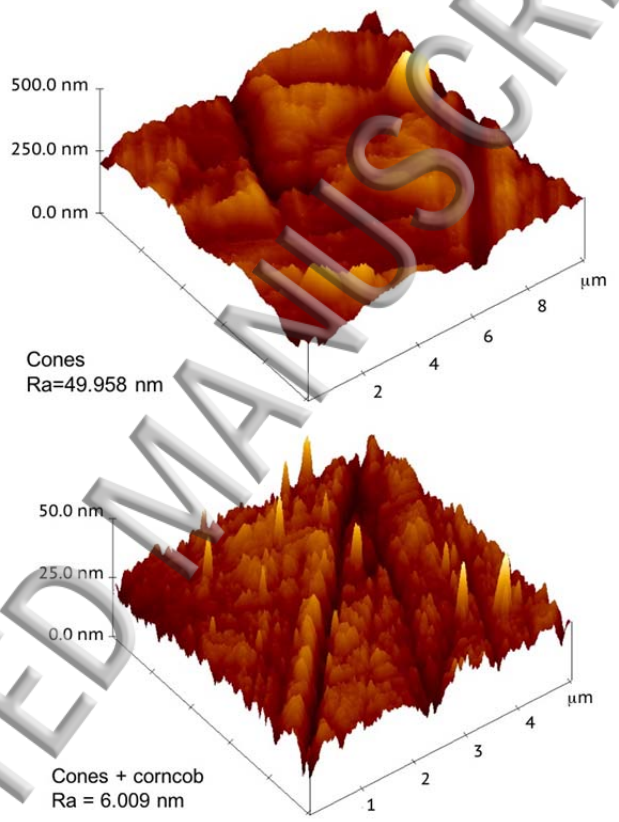

FIG. 6. Atomic force microscopy (AFM) surface analysis results of the square stainless steel coupons. Top: The surface finish Ra is ~ 50 nm after tumbling in plastic cones. Bottom: the surface finish Ra is ~ 6 nm after subsequent tumbling in corncob. The sampling area is ~ 25 um^2 for both images.

ACCEPTED MANUSCRIPT

AIP Publishing

This manuscript was accepted by Rev. Sci.Instrum. Click here to see the version of record.

Table 1. Roughness average (Ra) surface finish measurements of the 20 cm^2 stainless steel anode electrode disc, and 1 cm^2 stainless steel square coupons, compared to DPP-ed stainless steel parts described in Refs. 9 and 22. The Ra values of the coarse machined surfaces was too high to evaluate using the AFM.

Sample	Pre-CBP Ra (nm)	CBP Plastic cones Ra (nm)	CBP Plastic cones + corncob Ra (nm)	DPP Ra (nm)	Characterization method
20 cm^2 anode	185	182	76		Optical profilometry
1 cm^2 coupon	850 / NA	184 / 50	48 / 6		Optical profilometry / AFM
30 cm^2 electrode				30 [9]	Optical profilometry
7 cm^2 disc				4 [22]	AFM

ACCEPTED MANUSCRIPT

IV. PHOTOGUN ASSEMBLY AND HV CONDITIONING

The surface metrology results demonstrate that centrifugal barrel polishing with plastic cones and corncob media provides a mirror-like surface finish in hours, and comparable to the surface finish attained with diamond paste polishing techniques following weeks of intensive labor. However, the ultimate metric of success is the high voltage performance of the electrodes inside the dc high voltage photogun.

After manufacturing and vacuum degas at 900° C, each electrode was barrel polished, and finally cleaned in an ultrasonic bath of 2-propanol. The ceramic was thoroughly cleaned using lint-free wipes soaked in 2-propanol. The photogun was fully assembled in a class 1000 clean room. High pressure rinsing was not used on the electrodes, instead the insulator-electrode assembly was additionally cleaned using a CO_2 jet nozzle just prior to be integrated to the photogun vacuum chamber for minimizing the amount of dust particulates. After assembly, the photogun was moved to a radiation shielded test enclosure and vacuum baked at 200° C until the pressure drop was less than 10% in 24 hours. This occurred after ~ 300 hours. The NEG modules were activated at 450° C for 45 minutes at the end of the bake with the resulting vacuum in the low 10^{-11} Torr range.

Before a dc high voltage photogun can be used as an electron source, the electrodes must be high voltage conditioned. The purpose of high voltage conditioning is to render a photogun free of field emission when biased at the desired operating voltage. Field emitted electrons degrade the vacuum by desorbing gas (mainly hydrogen) upon impacting the vacuum chamber walls, and also generating x-rays that can stimulate unwanted photoemission, leading to catastrophic damage to the photogun when encountered at high levels.

AIP Publishing

This manuscript was accepted by Rev. Sci.Instrum. Click here to see the version of record.

The photogun was connected to a 500kV dc Cockcroft-Walton SF_6 gas–insulated high voltage power supply (HVPS), with a 300 MΩ conditioning resistor in series. Male-type cable connectors fit precisely into the conical inverted insulator on the photogun, and into a plastic receptacle supporting the conditioning resistor inside the HVPS SF_6 tank. The ceramic insulator, plastic receptacle and the high voltage cable are industry-standard components with dimensions specified by the commercial designation "R30".

Three signals related to field emission were monitored during conditioning: field emission current, photogun vacuum levels, and x-ray radiation levels. Ideally field emission current should be monitored with a floating ammeter in series with the conditioning resistor, but this configuration could not be easily implemented. Instead, field emission current was monitored as excess current from the power supply measuring stack above background levels that were benchmarked with the HVPS as a standalone system. The conditioning resistor limits the current that can be delivered in case of breakdown, and also protects the electrode via negative feedback – as current is drawn by excessive field emission, the voltage drop across the resistor reduces the voltage applied to the electrode. The cathode electrode is not protected from stored energy within the high voltage cable, downstream of the conditioning resistor.

Typical field emitters draw currents of tens of μA, but often sudden processing of an emitter tip (emitter burn-off) can result in a current surge up to 5 mA (the capacity of the HVPS), which can introduce breakdown at the insulator-cable plug, causing serious damage. To address this possibility, the HVPS current-limit was set to trip OFF voltage at 500 μA. In addition, x-ray dose measured in counts per second (CPS) by Geiger-Muller tubes (Gamma sensitivity Co60 18 CPS/mR/hr) placed around the gun vacuum chamber, and the vacuum levels measured by the photogun ion pump with a custom controller capable of reading ion current at the pico-Ampere level[24], were used to indicate the presence of field emission.

Initially, voltage was increased under vacuum conditions (~$3x10^{-11}$ Torr) at a rate of 10 kV/min up to 200kV, and then in steps of 5 kV at a rate of 1kV/min when the first vacuum disturbance was encountered, which was 225kV (~ 7 MV/m peak field) as shown by the green trace in figure 7. The x-ray radiation signal (orange data set) tracks the vacuum activity, with both signals indicating the signature of field emission. Voltage was increased slowly to process out field emitters, but the rate at which the voltage was increased depends on the vacuum level. It is important to let the vacuum recover to ~$1x10^{-10}$ Torr before increasing the voltage, to minimize the risk of developing new field emitters[7]. Literature indicates that a field emitter is eliminated when the electric field at the nm-size tip is sufficiently high to produce current density of the order 10^{12} A/m^2, which can slowly melt the tip producing a blunt topography[5,25]. The high current density can destroy the emitter, but also draw current that exceeds the current-limit of the HVPS (note the sharp drops in the HV signal of figure 7).

Field emission current levels upon restoring the voltage after the current-limit trip are usually lower, but in some instances higher, reaching hundreds of μA. When this happens, vacuum high voltage conditioning is not as effective. Rather, more importantly, vacuum high voltage conditioning is not as easy to control. An efficient complementary technique is gas high voltage conditioning. Krypton gas was added to the photogun vacuum chamber at pressure ~ $5x10^{-5}$ Torr, and then the voltage was raised from 0 to the last voltage setting reached under vacuum

ACCEPTED MANUSCRIPT

AIP Publishing

This manuscript was accepted by Rev. Sci.Instrum. Click here to see the version of record.

conditions at a rate of 100 kV/min, then more slowly at a rate of 0.5 kV/min[7]. Gas conditioning serves to eliminate stubborn field emitters through ion bombardment. Field emitted electrons ionize the gas resulting in localized sputtering of the emitter, and also suppressing field emission via ion implantation which serves to increase the local work function[26]. When radiation levels decrease to background levels (less than 5 CPS), the voltage was turned off, and the krypton gas pumped away. The vacuum recovers to nominal levels in a few hours since non-evaporable getter modules do not pump inert gases. Voltage could then be applied at a higher value. The photogun was then allowed to "soak" at high voltage under vacuum conditions for several hours. If more field emitters developed during the soak, gas conditioning was repeated.

The photogun was deemed conditioned at a particular voltage when radiation levels were indistinguishable from background levels. For example, even though the 350 kV target voltage was reached after ~ 60 hours, radiation levels were ~ 20 CPS higher than background, indicating that further gas conditioning at higher voltage was required. High voltage conditioning in the presence of krypton gas to 360 kV, and operation under vacuum conditions at 350 kV without field emission, took approximately 70 hours.

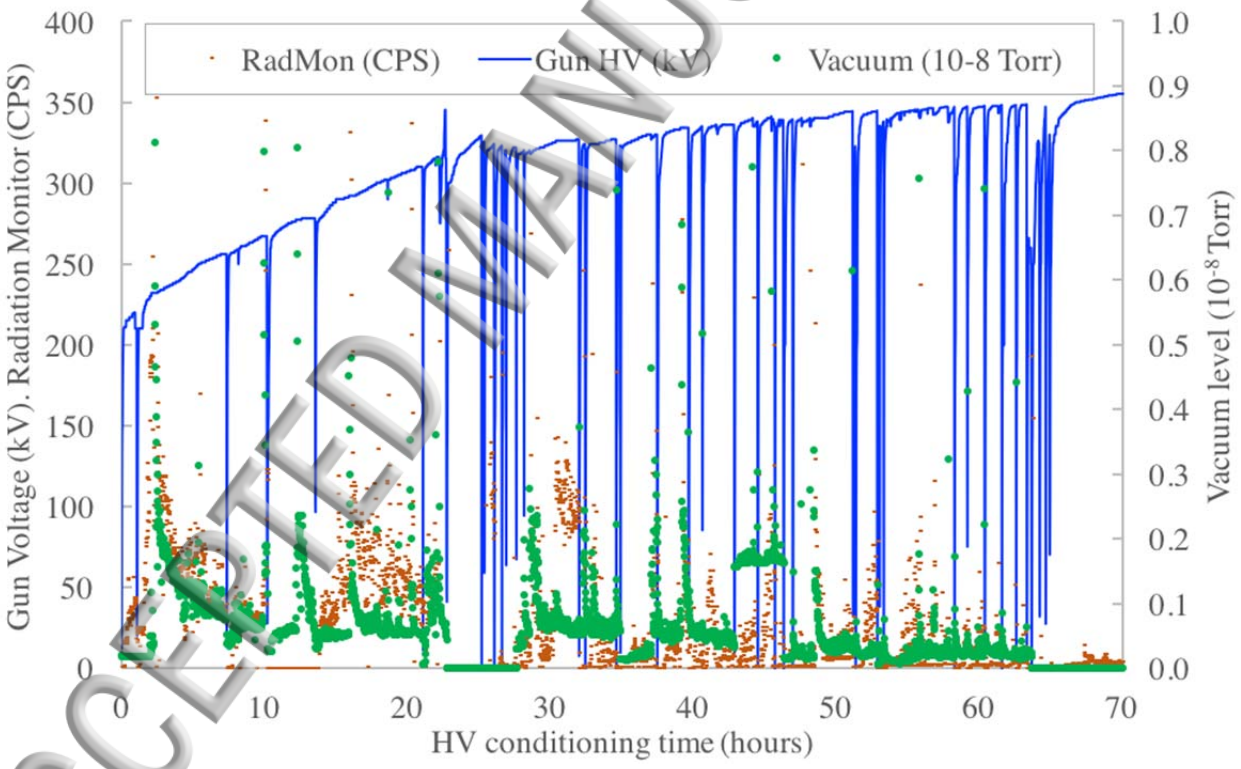

FIG. 7. Gun voltage (blue), vacuum level (green) and x-ray radiation level (orange) during high voltage conditioning to 360 kV. The pressure gets progressively lower as field emission if processed. Once conditioned, typical vacuum levels were ~ $3x10^{-11}$ Torr at 350 kV. Radiation levels also become progressively smaller as field emitters were processed out. At nominal 350 kV radiation levels were less than 10 CPS and comparable to background levels. Sharp vertical lines indicate the voltage tripping OFF, due to field emission current draw exceeding the current-limit setpoint of the HVPS.

ACCEPTED MANUSCRIPT

AIP Publishing

This manuscript was accepted by Rev. Sci.Instrum. Click here to see the version of record.

IV. CONCLUSIONS AND OUTLOOOK

We described a centrifugal barrel-polishing technique commonly used for polishing the interior surface of superconducting radio frequency cavities but implemented for the first time to polish stainless steel electrodes for dc high voltage photoguns. The technique reduced polishing time from weeks to hours while providing a mirror-like surface finish comparable to that obtained with labor intensive, skill-of-the-trade, diamond-paste polishing techniques. Since centrifugal barrel polishing relies on a machine with programmed settings, unprecedented consistency was obtained between different electrode samples, and electrode samples could not be damaged as a result of over-polishing.

A dc high voltage photogun based on an inverted-geometry insulator design was constructed using centrifugal barrel polished electrodes and standard high voltage dc photogun assembly techniques and procedures. It was tested to 360 kV, and demonstrated operation at 350 kV without field emission. The behavior of the centrifugal barrel polished electrodes during high voltage conditioning was similar to that observed in photoguns that employ DPP-ed or electropolished electrodes and large cylindrical ceramic insulators operating at higher voltages[10,12,13,14]. In contrast to such systems, higher voltage operation of the photogun presented in this work seems unrealistic considering the use of a cable and dimensions of the commercially available electrical components utilized in its construction. We also presented important design considerations related to the electrode shape and the electrode interface to the power supply particular to the inverted-insulator geometry employed at Jefferson Lab. This work represents the first implementation of the centrifugal barrel polishing techniques for the construction and operation of a compact 350 kV dc high voltage photogun.

V. ACKNOWLEDGEMENTS

The authors gratefully appreciate the efforts of C. Gould who characterized the barrel polished sample electrodes with the optical profilometer, P. Adderley who setup the photogun vacuum bake, and Dr. R. Suleiman for post-processing the photogun high voltage conditioning data.

Authored by Jefferson Science Associates, LLC under U.S. DOE Contract No. DE-AC05-06OR23177. The U.S. Government retains a non-exclusive, paid-up, irrevocable, world-wide license to publish or reproduce this manuscript for U.S. Government purposes

REFERENCES

[1] G. R. Neil, C. Behere, S. V. Benson, M. Bevins, G. Biallas, J. Boyce, J. Coleman, L. A. Dillon-Townes, D. Douglas, H. F. Dylla, R. Evans, A. Grippo, D. Gruber, J. Gubeli, D. Hardy, C. Hernandez-Garcia, K, Jordan, M. J. Kelley, L. Merminga, J. Mammosser, W. Moore, N. Nishimori, E. Pozdeyev, J. Preble, R. Rimmer, M. Shinn, T. Siggins, C. Tennant, R. Walker, G.

ACCEPTED MANUSCRIPT

AIP Publishing

This manuscript was accepted by Rev. Sci.Instrum. Click here to see the version of record.

P. Williams, S. Zhang, The JLab high power ERL light source, Nucl. Intstr. Meth. A 557 (2006) 9-15.
[2] E. J. Minehara, Development and operation of the JAERI superconducting energy recovery linacs, Nucl. Instr. Meth. A 557 (2006) 16-22.
[3] A. V. Fedotov for the LEReC team, Bunched Beam Electron Cooloing for the Low Energy RHIC Operation, ICFA Beam Dynamics Newsletter, No. 65, December 2014, pp. 22-27.
[4] R. G. Forbes, J. H. B. Deane, A. Fischer, and M. S. Mousa, Fowler-Nordheim Plot Analysis: a Progress Report, Jordan Journal of Physics, Vol. 8, No. 3, 2015, pp. 125-147.
[5] W. T. Diamond, New perspectives in vacuum high voltage insulation. I. The transition to field emission, J. Vac. Sci. Technol. A 16(2), Mar/Apr 1998, pp. 707-719.
[6] J. Grames, P. Adderley, J. Brittian, J. Clark, J. Hansknecth, D. Machie,M.Poelker, M. L. Stutzman, R. Suleiman and K. Surles-Law, Lifetime measurements of high polarization strained-superlattice gallium arsenide at beam current >1 milliamp using a new 100 kV load lock photogun, Particle Accelerator Conf., Albuquerque, NM, USA, pp. 3130-3132, 2007
[7] C. Hernandez-Garcia, S. V. Benson, G. Biallas, D. Bullard, P. Evtushenko, K. Jordan, M. Klopf, D. Sexton, C. Tennant, R. Walker, and G. Williams, dc high voltage conditioning of photoemission guns at Jefferson Lab FEL, AIP Conf. Proc. 1149, pp. 1071-1076, 2009.
[8] H. Tian, S. G. Corcoran, C. E. Reece, and M. J. Kelley, The Mechanism of Electropolishing of Niobium in Hydroflouric-Sulfuric Acid Electrolyte, Journal of the Electrochemical Society, 155 (9) D563-D568 (2008).
[9] M. BastaniNejad, A. A. Elmustafa, E. Forman, S. Covert, J. Hansknecht, C. Hernandez-Garcia, M. Poelker, L. Das, M. Kelley, P. Williams, Evaluation of electropolished stainless steel electrodes for use in DC high voltage photoelectron guns, J. Vac. Sci. Technol. A, Vol. 33, No. 4, Jul/Aug 2015.
[10] B. M. Dunham, and K. W. Smolenski, Design considerations for a high voltage DC photoemission electron gun at Cornell University, IEEE International Power Modulator and High Voltage Conference (IPMHVC), May 23-27 2010, Atlanta GA, USA, pp. 98-101.
[11] M. BastaniNejad, Md. Abdullah Mohamed, A. A. Elmustafa, P. Adderley, J. Clark, S. Covert, J. Hansknecht, C. Hernandez-Garcia, M. Poelker, R. Mammei, K. Surles-Law, and P. Williams, Evaluation of niobium as candidate electrode material for dc high voltage photoelectron guns, Phys. Rev. ST Accel. Beams **15**, 083502 (2012)
[12] N.Nishimori, R. Nagai, S. Matsuba, R.Hajima, M.Yamamoto, Y.Honda, and T. Miyajima, Experimental investigation of an optimum configuration for a high-voltage photoemission gun for operation at >500 kV, Phys. Rev. ST Accel. Beams, Vol. 17, 053401 (2014).
[13] J. Maxon, I. Bazarov, B. dunham, J. Dobbins, X.Liu, and K. Smolenski, "Design, conditioning, and performance of a high voltage, high brightness dc photoelectron gun with variable gap", Rev. Sci, Instrum. Vol. 85, 093306, 2014.
[14] C. Hernandez-Garcia, T. siggins, S. Benson, D. Bullard, H. F. Dylla, K. Jordan, C. Murray, G. R. Neil, M. Shinn, and R. Walker, A high average current dc GaAs photocathde gun for ERLs and FELs, Proceedings of the 2005 Particle Accelerator Conference, Knowxville, TN, USA, pp. 3117-3119, 2005.
[15] P. A. Adderley, J. Clark, J. Grames, J. Hansknecht, K. Surles-Law, D. Machie, M. Poelker, M. L. Stutzman, and R. Suleiman, Load-locked dc high voltage GaAs photogun with an inverted-geometry ceramic insulator, Phys. Rev. ST Accel. Beams 13, 010101 (2010).

ACCEPTED MANUSCRIPT

AIP Publishing

This manuscript was accepted by Rev. Sci.Instrum. Click here to see the version of record.

[16] P. Adderley, J. Clark, J. Grames, J. Hansknecht, M. Poelker, M. Stutzman, R. Suleiman, K. Surles-Law, J. McCarter, and M. BastaniNejad, CEBAF 200kV inverted electron gun, Proceedings of the 2011 Particle Accelerator Conference, New York, NY, USA, pp. 1501-1503, 2011.
[17] C. Hernandez-Garcia, M. Poelker, and J. Hansknecht, High Voltage Studies of Inverted-geometry Ceramic Insulators for a 350kV DC Polarized Electron Gun, IEEE, Trans. Diel. Elec. Insul., Vol 23, No. 1, Feb. 2016, pp. 418-427
[18] Société des Céramiques Techniques, SCT, https://www.sct-ceramics.com/en/.
[19] J. Grames, P. Adderley, J. Brittian, J. Clark, J. Hansknecht, D. Machie, M. Poelker, E. Pozdeyev, M. Stutzman, and K. Surles-Law, A Biased Anode to Suppress Ion Back-Bombardment in a DC High Voltage Photoelectron Gun, 2008 AIP Conf. Proc. **980** 110.
[20] K. Halbach, "LANL SUPERFISH", Lawrence Livermore National Laboratory Technical Report No. UCRL-17436, 1967.
[21] Mass Finishing, Inc., http://www.massfin.com.
[22] N. D. Theodore, B. C. Holloway, D. Manos, R. Moore, C. Hernandez, T. Wang, and H. F. Dylla, Nitrogen-Implanted Silicon Oxynitride: A Coating for suppressing Field Emission From Stianless Steel Used in High-Voltage Applications, IEEE Transactions on Plasma Science, Vol. 34, No. 4, August 2006, pp. 1074-1079.
[23] C. Y. Poon, and B. Bhushan, Comparison of surface roughness measurements by stylus profile, AFM and non-contact optical profile, Wear (an international journal on the science and technology of friction, lubrication and wear by Elsevier) 190 (1995) pp. 76-88.
[24] J. Hansknecht, "Model EOS-902 UHV Ion Pump Controller Technical Manual ", https://wiki.jlab.org/ciswiki/images/f/f7/EOS_902_tech_manual.pdf
[25] R. V. Latham, High Voltage Vacuum Insulation, 2nd ed. (Academic, London, 1995).
[26] M. BastaniNejad, A. A. Elmustafa, E. Forman, J. Clark, S. Covert, J. Grames, J. Hansknecht, C. Hernandez-Garcia, M. Poelker and R. Suleiman, Improving the performance of stainless-steel DC high voltage photoelectron gun cathode electrodes via gas conditioning with helium or krypton, Nucl. Instr. and Meth. in Phys. Res. A, Vol. 762, pp. 135–141, 2014

ACCEPTED MANUSCRIPT

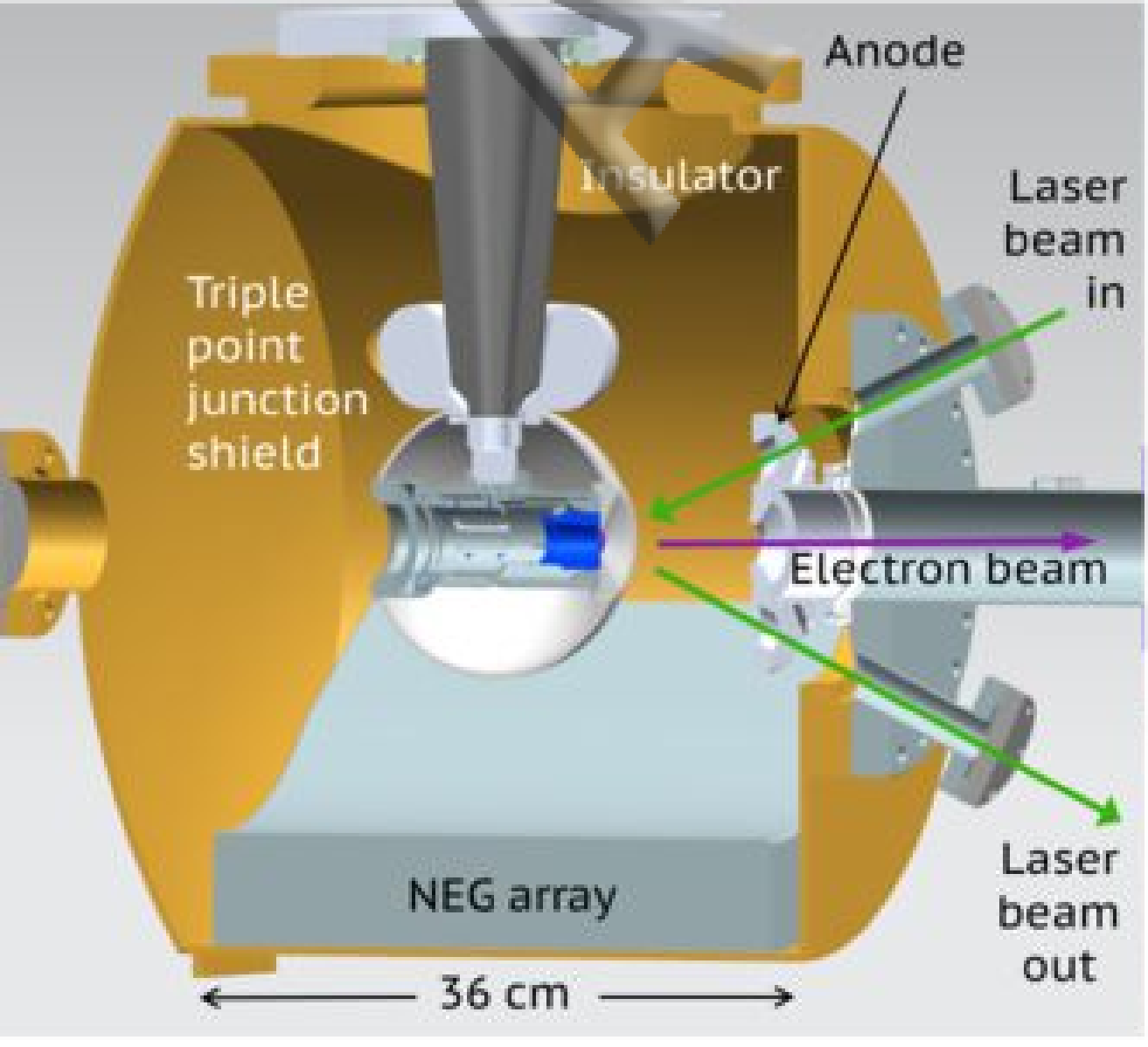
Anode
Insulator
Laser
beam
in
Triple
point
junction
shield
Electron beam
Laser
beam
out
NEG array
36 cm

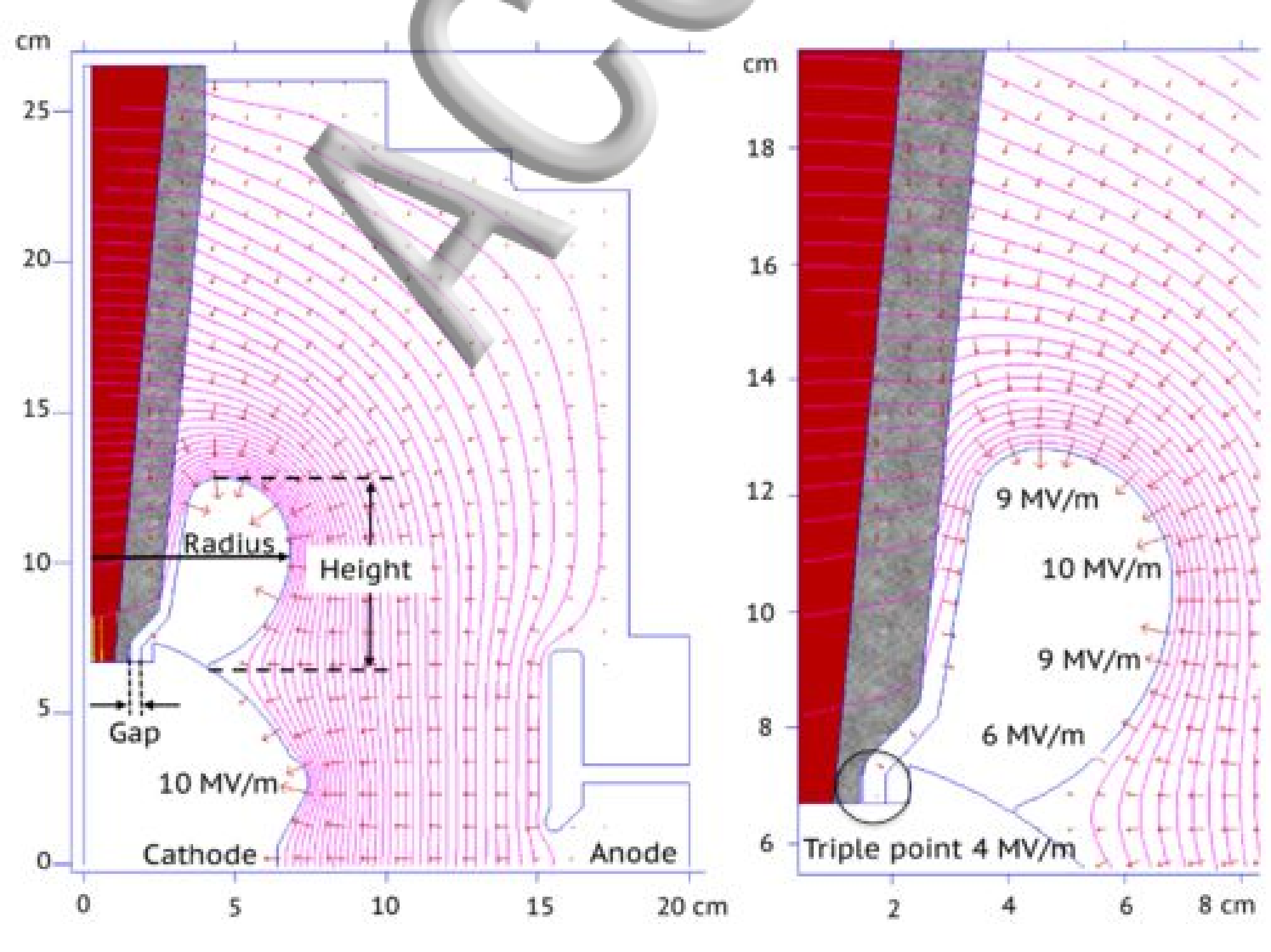
cm
25
20
15
10
5
0
Radius
Height
Gap
10 MV/m
Cathode
Anode
0
5
10
15
20 cm
cm
18
16
14
12
10
8
6
9 MV/m
10 MV/m
9 MV/m
6 MV/m
Triple point 4 MV/m
2
4
6
8 cm

AUTHORIZED USERS
ONLY
Training Required
DANGER

MADE IN U.S.A
NO.R 501-12
2
3
4

ACCEPTED

ACCEPTED

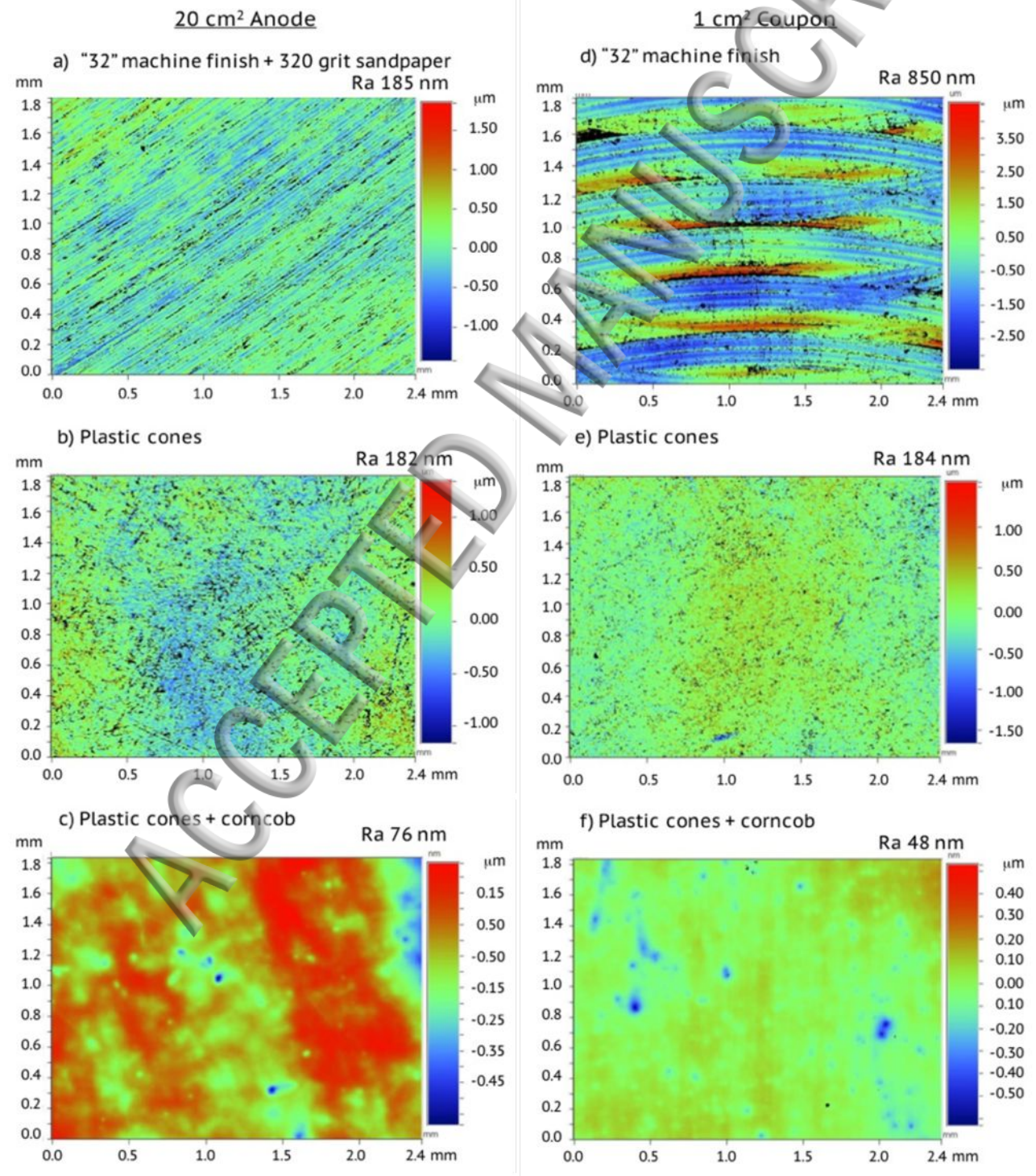

ACCEPTED MANUSCRIPT

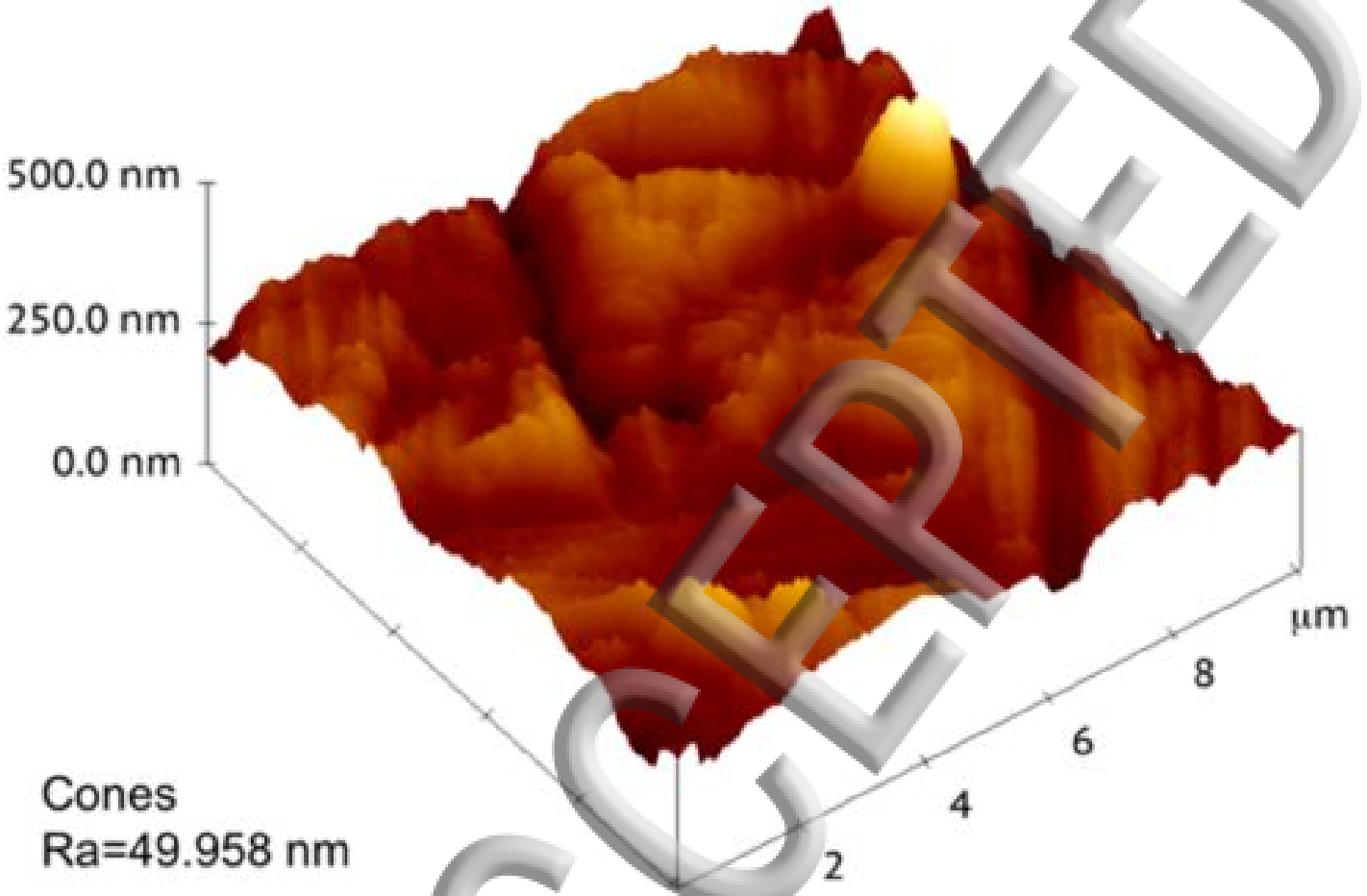

Cones
Ra=49.958 nm

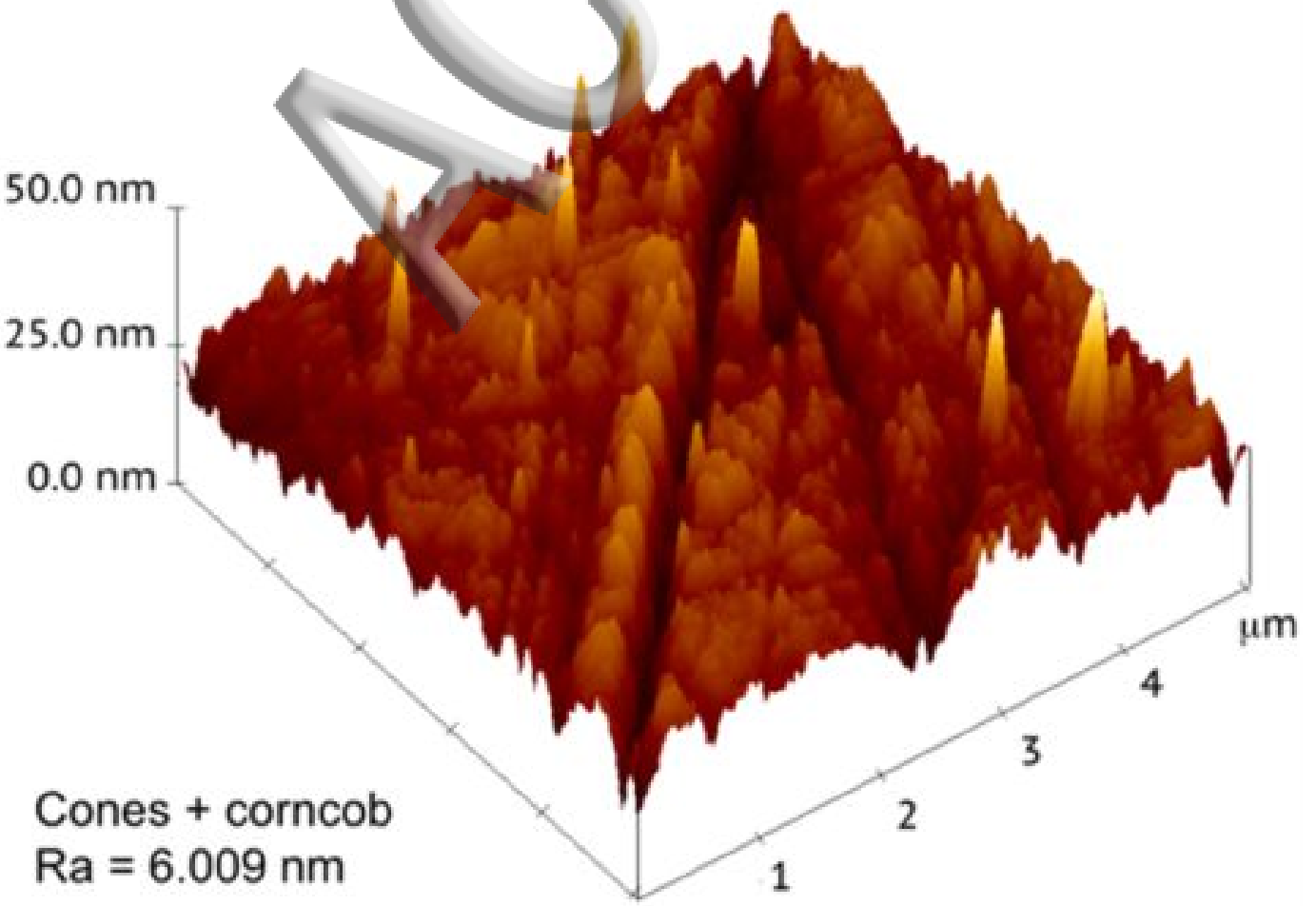

Cones + corncob
Ra = 6.009 nm

ACCEPTED

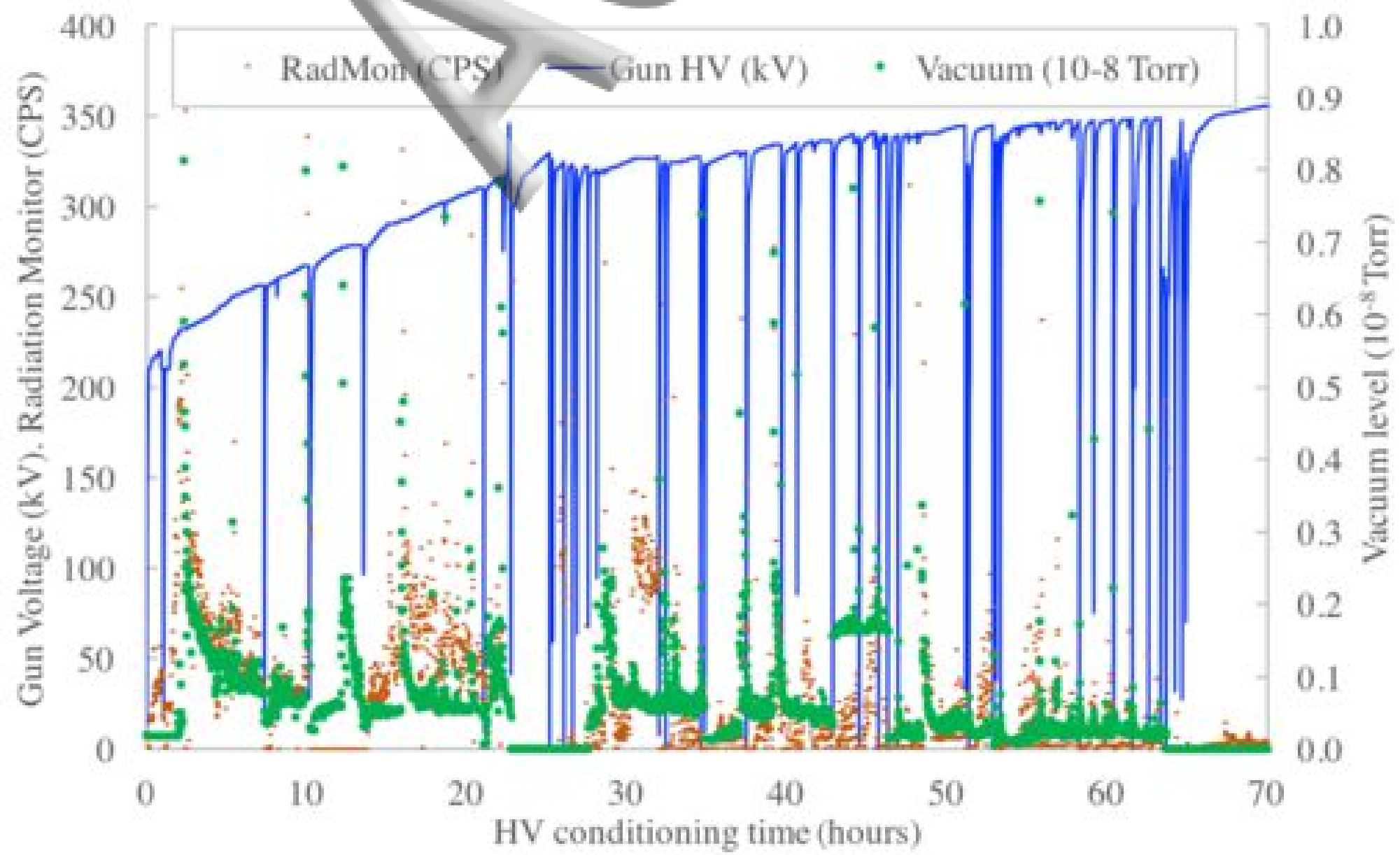
RadMon (CPS)
Gun HV (kV)
Vacuum (10-8 Torr)
Gun Voltage (kV), Radiation Monitor (CPS)
Vacuum level (10-8 Torr)
HV conditioning time (hours)
0
50
100
150
200
250
300
350
400
0.0
0.1
0.2
0.3
0.4
0.5
0.6
0.7
0.8
0.9
1.0
0
10
20
30
40
50
60
70